A Surprising Role for Conformational Entropy in Protein Function

A. Joshua Wand, Veronica R. Moorman, and Kyle W. Harpole

Abstract Formation of high-affinity complexes is critical for the majority of enzymatic reactions involving proteins. The creation of the family of Michaelis and other intermediate complexes during catalysis clearly involves a complicated manifold of interactions that are diverse and complex. Indeed, computing the energetics of interactions between proteins and small molecule ligands using molecular structure alone remains a great challenge. One of the most difficult contributions to the free energy of protein–ligand complexes to access experimentally is that due to changes in protein conformational entropy. Fortunately, recent advances in solution nuclear magnetic resonance (NMR) relaxation methods have enabled the use of measures-of-motion between conformational states of a protein as a proxy for conformational entropy. This review briefly summarizes the experimental approaches currently employed to characterize fast internal motion in proteins, how this information is used to gain insight into conformational entropy, what has been learned, and what the future may hold for this emerging view of protein function.

Keywords Binding free energy · Conformational entropy · Drug design · Michaelis complexes · Molecular recognition · Motional proxy · NMR relaxation

Contents

A.J. Wand (✉), V.R. Moorman, and K.W. Harpole
Graduate Group in Biochemistry & Molecular Biophysics, The Johnson Research Foundation and Department of Biochemistry & Biophysics, University of Pennsylvania Perelman School of Medicine, Philadelphia, PA 19104-6059, USA
e-mail: wand@mail.med.upenn.edu

Abbreviations

CaM	Calcium-saturated calmodulin
CaMK1(p)	CaM-binding domain of the calmodulin kinase I
CaMKKα(p)	CaM-binding domain of calmodulin kinase kinase alpha
CSA	Chemical shift anisotropy
DHF	Dihydrofolate
DHFR	Dihydrofolate reductase
eNOS(p)	CaM-binding domain of the epithelial nitric oxide synthase
	GlcNAc N-acetyl-D-glucosamine
HEWL	Hen egg white lysozyme
J(ω)	Lipari–Szabo model-free spectral density at frequency ω
NADPH/NADP$^+$	Reduced/oxidized nicotinamide adenine dinucleotide phosphate
NMR	Nuclear magnetic resonance
nNOS(p)	CaM-binding domain of the neuronal nitric oxide synthase
	NOE Nuclear Overhauser effect
O^2	Lipari–Szabo model free squared generalized order parameter
PDE(p)	CaM-binding domain of the phosphodiesterase
smMLCK(p)	CaM-binding domain of the myosin light chain kinase
SW	Square well potential energy function
T_1 (R_1)	Longitudinal relaxation time (longitudinal relaxation rate)
T_2 (R_2)	Transverse relaxation time (transverse relaxation rate)
ΔS_i	Change in entropy for the ith component
τ_e	Lipari–Szabo model-free effective correlation time
τ_m	Isotropic macromolecular tumbling correlation time

1   Introduction

Molecular recognition by proteins is fundamental to almost every biological process, particularly those protein–ligand complexes underlying enzymatic catalysis. The process of molecular recognition has therefore been of central interest from the earliest days of enzymology. Various mechanistic frameworks have been

constructed to describe the physical basis for specific high affinity interactions between protein molecules and their ligands. They have ranged from the simple "lock and key" interaction model [1] to the "induced fit" [2] and the more recent "conformational selection" models [3, 4]. Each of these derives from an increasing recognition of the plasticity and energetics of the ensemble of structures that proteins occupy [5, 6] and the potential role for travelling across this complex energy landscape in protein function [7, 8].

For the most part, the predominant interest has been in characterizing how motion between structural states correlate with protein function. There have been spectacular demonstrations of conformational selection (e.g., [9, 10]) and strong indications for the participation of "special" protein motions in catalysis by enzymes (e.g., [11–14]), though the latter role has been vigorously criticized on general principles [15] (but see [16]). What concerns us here is not that proteins move from one functional state to another but rather what is the thermodynamic basis of these functionally relevant states. This is a long-standing issue and is intimately related to the so-called protein folding problem and the free energy landscape that protein molecules explore [17]. Stated less obliquely, we wish to understand the physical basis for the (de)stabilization of a given state of a protein molecule. Perhaps the most primitive and potentially simplest function that a protein engages in is high affinity molecular recognition. The formation of protein complexes involves a complicated manifold of interactions that are diverse and complex. This complexity is reflected in the difficulty of computing the energetics of interactions involving proteins using molecular structure alone [18–20]. Indeed, structure-based design of pharmaceuticals has been impeded by this barrier [21]. Here, we specifically focus on the role of protein conformational entropy in modulating the free energy of the association of a protein with a ligand.

Expression of the total binding free energy emphasizes that the entropy of binding is comprised of contributions from the protein, the ligand and the solvent:

$$\Delta G_{bind} = \Delta H_{bind} - T(\Delta S_{protein} + \Delta S_{ligand} + \Delta S_{solvent}) \tag{1}$$

The free energy of binding (ΔG_{bind}) and the enthalpy of binding (ΔH_{bind}) can in favorable cases be directly measured using isothermal titration calorimetry [22] and the associated total binding entropy (ΔS_{bind}) obtained by arithmetic. Unfortunately, as (1) indicates, the molecular origins of these thermodynamic parameters remain obscure. Views of associations involving proteins have largely been seen through the lens of enthalpy owing to the richness of our knowledge of the structure of proteins and their complexes, which helps reveal the details of the interactions governing the enthalpy. In great contrast, the origin of the change in entropy remains difficult to grasp as it inherently involves a manifold of states that the protein, ligand, and solvent can occupy, each having its own probability for existence. Historically, the contributions by solvent entropy to binding thermo-dynamics have taken center stage and are usually framed in terms of the hydrophobic effect [23]. Hydrophobic solvation by water continues to be the subject of extensive analysis [24, 25].

In principle, the entropic contribution of a structured protein to the binding of a ligand ($\Delta S_{\mathrm{protein}}$) includes both changes in its internal conformational (configurational) entropy (ΔS_{conf}) and changes in rotational and translational entropy (ΔS_{RT}) [26]. Equation (1) emphasizes that the measurement of the entropy of binding does not resolve contributions from internal protein conformational entropy. Arguments from fundamental theory [27] and observations from simulation (e.g., [28, 29]) and experiment (e.g., [30, 31]) in the 1970s indicated that proteins fluctuate about a structure closely similar to that observed by crystallography and that these fluctuations could reflect significant residual conformational entropy. Yet it is only recently that experimental methods and strategies have been created to assess this and related ideas quantitatively.

Experimental measurement of ΔS_{conf} has been difficult. During the past decade, we and others have been developing NMR methods that serve to provide measures of motion between different microscopic structural states and thus can act as an indirect measure of or proxy for conformational entropy [32]. The idea is simple, but extremely tricky to implement. However, as outlined below, solution NMR spectroscopy has emerged as the most powerful experimental technique for accessing protein motion in a site-resolved comprehensive manner. Motion expressed on the sub-nanosecond time scale corresponds to significant entropy [33, 34] and NMR relaxation methods are particularly well suited for its characterization [32]. As will be illustrated in detail below, this leads directly to the idea of using measures of motion as a proxy for conformational entropy. Thus, detection of motion segues into the issue of conformational entropy, though it is not obvious how to employ measures of motion as a quantitative measure of conformational entropy. Of course, one must first enable the site resolved measurement of internal motion (disorder) of proteins.

2 Solution NMR Spectroscopy and Detection of Motion

Over the past two decades, solution NMR spectroscopy has emerged as a powerful means for the site-resolved measurement of motion on an impressive range of time scales in proteins of significant size [32, 35–37]. The breadth of available time scales is daunting and leaves one asking where, with limited resources, one should begin. Here we are ultimately most focused on those motions that *express* large contributions to protein conformational entropy. Simple arguments suggest that this should be largely manifested in the extremely fast motions corresponding to bond vibrations and torsional oscillations, which generally occur on the nanosecond and faster time scales [33]. Classical NMR relaxation phenomena allow access to this time scale.

Very briefly, an ensemble of nuclear spins can relax from a non-equilibrium state via a range of potential interactions. For example, the inter-nuclear dipole–dipole interaction between spatially proximal hydrogens gives rise to the nuclear Overhauser effect (NOE), which is likely familiar to the non-expert reader as a

means to measure inter-atomic distances for the determination of molecular structure in solution. The strength of this interaction depends on the time average of the distance between the nuclei and of the angle of the inter-nuclear vector with the applied magnetic field. In favorable situations, such as when the two nuclei are bonded, the distance dependence is effectively constant (though see [38, 39]) and the interaction is temporally modified only by the change in the orientation of the bond vector with respect to the magnetic field. Examples include the ^{15}N–^1H amide bond and the ^{13}C–^1H bond in a variety of contexts such as in a methyl group. Other nuclear spin interactions are perhaps more obscure to the reader and include chemical shift anisotropy (CSA), which reflects the interaction of the nuclear spin with the asymmetric distribution of electrons about it, and the electrostatic interaction between the quadrupolar moment of a nucleus having a spin quantum number of one or greater and the surrounding electric field gradient. In some cases, the "interference" or "cross correlation" between different relaxation mechanisms can offer insight into motion (e.g., [40–45]), though these approaches are not common owing to a variety of technical limitations.

Relaxation of nuclear spins in liquid samples to an equilibrium distribution of spin states is mediated by the fluctuation of local fields. Rapid molecular motions impose time modulation on these local fields and it is through this dependence that information about motion can be obtained. The theoretical treatment of the connection between motion and NMR relaxation phenomena is complicated. The interested reader is referred to a recent monograph on this and related subjects [46]. A popular and very robust way of capturing the essential character of the motion that gives rise to NMR relaxation phenomena of the type considered here is the so-called model free approach of Lipari and Szabo [47, 48]. The various NMR observables that can be measured can be generally expressed as linear combinations of the so-called spectral density functions. The spectral densities are in turn defined by the motion of the "interaction" vector within the protein. Consider a ^{13}C nucleus attached by a single ^1H, i.e., in a CHD_2 isotopomer. The deuterium nucleus has a much weaker interaction than the ^1H nucleus and its effects can be largely ignored (though they are not in the final analysis). The motion of the ^{13}C–^1H interaction vector (in this case along the rigid bond between them) can be described by an autocorrelation function, which is simply the dot product of the interaction vector's orientation at some time t and its orientation at some time t'. The time dependence will have two components: a contribution from the slower global tumbling of the protein and an assumed faster component due to motion within the molecular frame. In the simplest case, the Lipari–Szabo treatment leads to three parameters: a correlation time for isotropic macromolecular reorientation (τ_m), an effective correlation time (τ_e), and a measure of the angular disorder of the interaction vector termed the squared generalized order parameter (O^2).[1] The order parameter by definition ranges from zero to one, corresponding to complete isotropic disorder

---

[1] Please note: to avoid confusion with entropy we will refer to the Lipari–Szabo squared generalized order parameter as O^2 rather than its original designation as S^2.

and complete rigidity of the interaction vector within the molecular frame, respectively. It is this motional parameter that offers the potential to provide access to statements about conformational entropy. The effective correlation time has a strong technical definition that precludes its general use as faithful descriptor of the time constant(s) for the underlying motion.

The Lipari–Szabo model-free spectral density has a very simple form:

$$J(\omega) = \frac{O^2 \tau_m}{1 + \omega^2 \tau_m^2} + \frac{(1 - O^2)\tau}{1 + \omega^2 \tau^2} \tag{2}$$

where $\tau^{-1} = \tau_m^{-1} + \tau_e^{-1}$. The spectral densities are linearly combined as required by the physics of the specific NMR relaxation mechanism to define an observable relaxation (see [32] for illustrative derivations). For example, the longitudinal relaxation rate ($1/T_1$ or R_1) of the ^{13}C nucleus by a single bonded ^{1}H nucleus is given by:

$$R_1 = \frac{d^2}{4}[J(\omega_H - \omega_C) + 3J(\omega_C) + 6J(\omega_H + \omega_C)] \tag{3}$$

where d^2 is comprised of fundamental constants and the effective C–H bond length and ω_H and ω_C are the resonance frequencies of ^{1}H and ^{13}C nuclear spins, respectively. For each site of interest there are two unknowns (O^2 and τ_e) plus one global variable (τ_m) defining isotropic tumbling of the protein in solution. The situation can become more complicated, of course. For example, the character of the tumbling of the macromolecule may be anisotropic to some degree. This is easily handled using appropriate diffusion equations and data filtering [49–52].

Similarly, specific instances may require (justify) more or less complex forms of the model-free spectral density shown above [53]. Nevertheless, the experimental prescription is clear: resolve relaxation data at n individual sites in a protein and measure as many relaxation parameters (e.g., T_1, T_2, etc.) at as many magnetic fields (to vary ω_H, ω_C) as needed to provide a robust determination of the $2n + 1$ (in the case of isotropic macromolecular tumbling) parameters.

Several key steps were required to enable the comprehensive use of NMR relaxation phenomena to characterize the internal motion of proteins of significant size. The advent of multidimensional NMR spectroscopy provides a means to resolve literally hundreds of probe sites for motion in proteins. Sophisticated isotopic labeling schemes have been introduced to simplify the complexity of the NMR relaxation as much as possible in order to make its measurement and subsequent analysis more robust (e.g., [54–60]). Generally, the strategy is to reduce the number of relaxation mechanisms (interactions) as much as possible. Finally, the cornerstone was the development of NMR experiments that prepared "pure" NMR observables of NMR relaxation that could be directly interpreted. Lewis Kay and colleagues are largely identified with the development of the NMR machinery necessary to measure ^{15}N [61, 62], ^{2}H [63, 64], and ^{13}C [65] autorelaxation in proteins. More recently, Tugarinov and coworkers have extended the number of
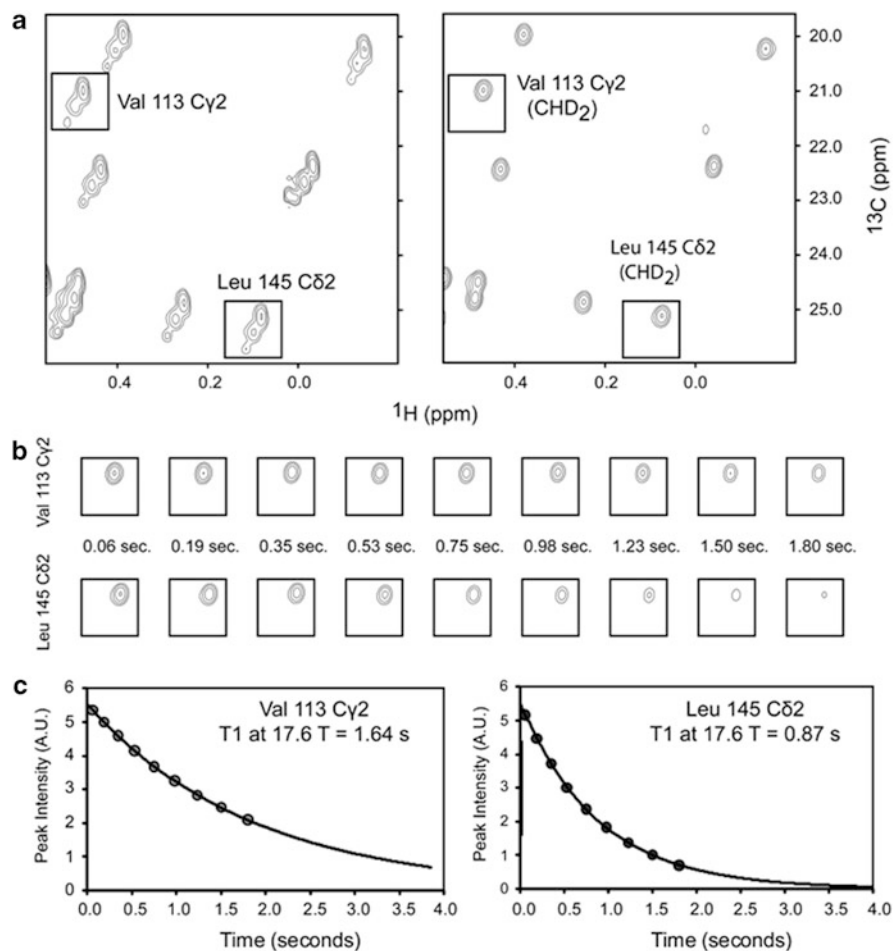
Fig. 1 Observation of carbon relaxation in proteins. (**a**) Protein is expressed during growth on $^{13}CHD_2COOD$ pyruvate in D_2O. Most methyl groups are selectively labeled with ^{13}C [57] as a mixture of deuterium isotopomers [67]. (**b**) The appropriate $^{13}CHD_2$ methyl isotopomer is selected during preparation of magnetization which (**c**) allows longitudinal and transverse relaxation to be measured in an otherwise deuterium background [65]. See [32] for further details

deuterium relaxation experiments that provide a context for extracting even more fundamental relaxation rate constants at a single magnetic field [66]. Notable contributions for implementing ^{13}C relaxation in the context of proteins came from Torchia and colleagues in their unraveling of the complexity of this particular mechanism of relaxation [67]. Finally, computational strategies were needed to extract confidently the desired model-free parameters [53, 68, 69].

The basic experimental strategy is outlined for methyl carbon relaxation in Fig. 1. To make this particular situation as simple as possible, the interaction of the methyl carbon is restricted to a single bonded ^1H. This is arranged by expression

of the protein of interest during growth on randomly partially deuterated $^{13}C_3$-pyruvate as a general carbon source [57] or with unlabeled glucose and appropriately labeled metabolic precursors for valine, leucine, and isoleucine [59]. Protein expression is carried out in "100%" D_2O to ensure elimination of ^1H spins at non-methyl sites in the protein [67].

Proteins produced in this manner are largely deuterated with selective ^1H and ^{13}C labeling in methyl groups. The methyl groups are mixtures of isotopomers (i.e., CD_3, CHD_2, CH_2D, CH_3). Only the three carrying at least one hydrogen are observed in the two-dimensional $^1H–^{13}C$ chemical shift correlation spectrum (Fig. 1). The three observed isotopomers give crosspeaks that are at slightly different positions in the spectrum. The appropriate isotopomer, in this case the CHD_2, is selected by spectroscopic manipulation [65]. The NMR relaxation experiment is designed to follow the return of a particular type of magnetization from a non-equilibrium state back to equilibrium. For carbon relaxation in proteins, longitudinal and transverse relaxation processes are most useful and are likely familiar to the non-specialist reader as "T_1" and "T_2" relaxation, respectively. The NOE is not so useful in the context of carbon relaxation in proteins of significant size since this observable reaches a limit as molecular tumbling slows. The relaxation process at a given methyl is quantified by the variation of the intensity of the corresponding $^1H–^{13}C$ cross peak with the relaxation time period (Fig. 1). The variation of the rate of relaxation across sites in the protein reveals corresponding differences in the underlying dynamics.

3 Fast Motion in Proteins Observed by NMR Relaxation

For technical reasons alluded to above, the primary probes of fast ps–ns motion in proteins have been the amide N–H bond and the C–H bond in methyl groups. Here "fast" is defined by processes occurring on time scales significantly shorter than the macromolecular tumbling time of the protein in solution, which is generally on the order of 50 ns or less in the context of current studies. The ^{15}N experiments are relatively straightforward and there are literally hundreds of studies of proteins spanning a significant range of topologies and contexts [36]. The view of the backbone provided by amide ^{15}N relaxation is generally unimpressive with uniformly high order parameters (rigidity) in regions of large elements of regular secondary structure (i.e., beta sheets, helices), which are bounded by the termini and intervening loops, turns, and sections of irregular structure having significantly larger amplitude motion [36]. Changes in functional state generally have small and often quite subtle effects on the backbone of the protein. Overall, the polypeptide chain appears largely to be a relatively rigid scaffold. Most of the dynamic response in the ps-ns time regime to changes in functional state is seen to reside in the side chains [32]. Observation of methine and methylene carbon hydrogens is complicated by the difficulty of appropriate labeling [55, 56, 70]. For probing the motion of methyl-bearing amino acid side chains, deuterium relaxation is preferred due to
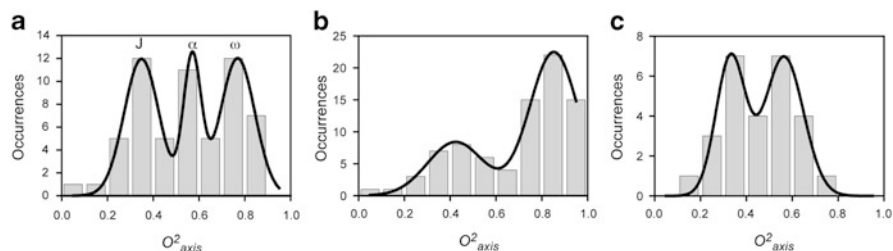
Fig. 2 Histograms of the distribution of squared generalized order parameters of methyl group symmetry axes (O^2_{axis}) in (**a**) the complex of calcium-saturated calmodulin and a peptide derived from the calmodulin-binding domain of the smooth muscle myosin light chain kinase [72], (**b**) flavodoxin [73], and (**c**) α_3D, a protein of de novo design [74]. *Lines* are best fits to a sum of three Gaussians. Taken from Igumenova et al. [32]. Copyright American Chemical Society

the purity of the source of its relaxation [32]. However, again for technical reasons, this approach is largely restricted to proteins smaller than ~25 kDa due to the effects of slow macromolecular reorientation in solution. For larger proteins, carbon relaxation methods prove to be the most robust though preparation of the samples and analysis of the data is somewhat more involved [67, 71]. The motion of methyl-bearing side chains in several dozen proteins have been studied in comprehensive detail using these methods [32]. Though sometimes obscured due to limited sampling in small proteins, three types or classes of motion of methyl-bearing side chains have been revealed by the distribution of methyl symmetry axis Lipari–Szabo order parameters [32]. The so-called J-class is centered around an O^2_{axis} value of ~0.35 and involves motion of the methyl group between rotameric wells, leading to averaging of the associated J-coupling. The α-class is centered around an O^2_{axis} value of ~0.65 and has smaller contribution from motions that lead to rotameric interconversion and generally reflects large amplitude motion within a single rotameric well. The ω-class is centered around an O^2_{axis} value of ~0.85 and has highly restricted motion within a single rotameric well that is somewhat reminiscent of the uniform rigidity of most backbone sites.

What is fascinating about these classes of motion is that their distribution in individual proteins can be quite variable (Fig. 2). The significant variation in the effective amplitude of motion through the protein matrix is perhaps somewhat counterintuitive. For example, restriction of motion is not strongly correlated with the depth of burial and other simple structural features [32]. Clearly, the "rules" for motion in proteins remain to be fully understood.

4 Motional Proxy for Conformational Entropy

Some time ago Akke and coworkers [75] introduced a theoretical scheme that provided a parametric connection between motion captured by NMR relaxation and the thermodynamic parameters of an ensemble of motional probes. This is

directly revealed by the formal definition of the Lipari–Szabo squared generalized order parameter [47]:

$$O^2 = \int\int p_{\text{eq}}(\Omega_1)P_2(\cos\theta_{12})p_{\text{eq}}(\Omega_2)\mathrm{d}\Omega_1\,\mathrm{d}\Omega_2 \tag{4}$$

where Ω_1 and Ω_2 represent separate orientations (states) of the NMR interaction vector, p_{eq} is the corresponding probability of each state, and P_2 the second order Legendre polynomial of the cosine of the angle θ_{12} between the two states. Clearly, the explicit consideration of the probability of the various states accessible to the NMR relaxation probe provides a direct connection to the partition function governing the ensemble. Hence, in principle, one can have access to the fundamental thermodynamic parameters of the ensemble through the usual relations. However, this approach requires a specific model (potential energy) for the motion in order to make the parametric connection between what can be measured (O^2) and what is desired (S).

Adopting this idea, we [34] and Yang and Kay [76] used the simple harmonic oscillator and diffusion in an infinite square well potential, respectively, to illustrate the parametric relationship between the Lipari–Szabo squared generalized order parameter (O^2) and entropy (S). The uses of motion as a proxy for or as an indirect measure of conformational entropy and some of the fundamental issues associated with this strategy are illustrated in Fig. 3. Consider an amino acid side chain with a single degree of motional freedom such as a point about which the side chain can pivot. Three different simple potentials based on the angle of the pivot are illustrated in Fig. 3. The square well potential has an infinite barrier set at some fluctuation angle. This potential corresponds to free diffusion in a cone, which has an analytical expression relating the Lipari–Szabo order parameter to the corresponding entropy [76]. This infinite square well potential is somewhat unrealistic as it does not express thermodynamic some properties such as heat capacity, which are an essential descriptor of protein molecules [77].

Also illustrated in Fig. 3 are the classic quadratic harmonic oscillator and its stiffer sixth power colleague, which do have the ability to represent a broader range of thermodynamic attributes of proteins in this context [75, 78]. The family of potentials of Fig. 3 gives entropies that are off-set from each other. Given the persistent uncertainty of the precise nature of the potential governing protein motion, the determination of *absolute* entropy is generally not possible. Fortunately, as Fig. 3 also indicates, the dependence of the slope (i.e., $\mathrm{d}S/\mathrm{d}O^2$) is relatively insensitive to the nature of the underlying potential. Thus *differences* in entropy obtained from *differences* in measures of motion seems to be possible [34]. Thus the "dynamical proxy" for entropy would appear to be useful for analysis of changes in motion corresponding to variation of the Lipari–Szabo order parameter between ~0.1 and ~0.9 even in the presence of a possible change in the underlying potential energy function upon a change in state (e.g., a binding event, pressure and temperature change, etc.).
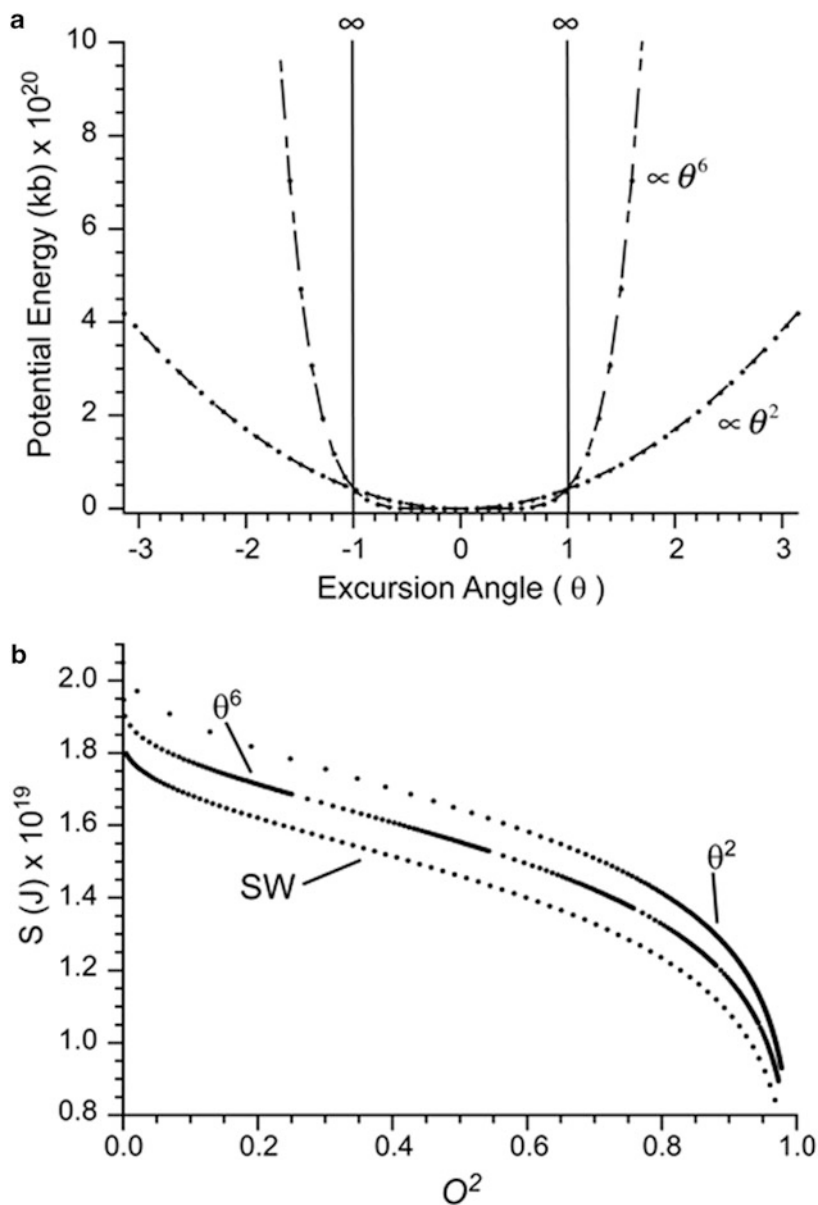
Fig. 3 The dynamical proxy for entropy. (**a**) Various simple potential energy functions governing the behavior of an attached NMR relaxation "spy". Shown are the infinite square well potential (*SW*) with an angular barrier of 1 radian, the simple harmonic oscillator potential with a quadratic dependence on the excursion angle (θ^2) and its sixth-power cousin (θ^6). (**b**) Parametric relationships between the various potentials and the corresponding Lipari–Szabo squared generalized order parameter. See [34, 75, 76, 78] for further explanation and examples
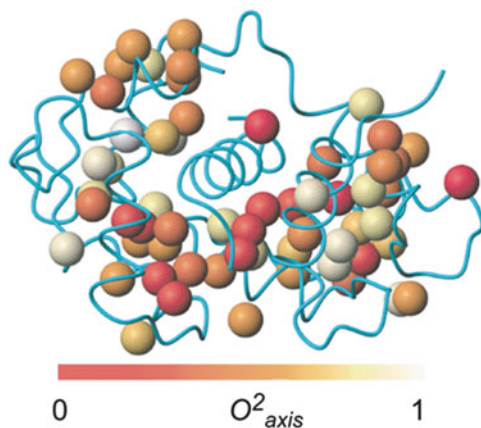
Fig. 4 *Ribbon* representation of the complex of calcium-saturated calmodulin and a peptide corresponding to the calmodulin-binding domain of the calmodulin kinase I. Methyl groups of calmodulin are represented as *spheres* and are shaded according to Lipari–Szabo order parameter of the methyl symmetry axis (O^2_{axis}) as determined by deuterium relaxation methods. Taken from Frederick et al. [91]. Copyright American Chemical Society

In an approach that we term an "oscillator inventory," a simple prescription is used to estimate changes in conformational entropy from changes in protein internal motion: (1) measure as many differences in Lipari–Szabo order parameters between two states of the protein as possible; (2) look-up the corresponding changes in entropy (i.e., using the type of relationship shown in Fig. 3); and (3) take the differences and simply add them up. There are many legitimate objections to this approach, including concerns about correlated motion, incomplete sampling, validity of the potential, the dependence of the observed relaxation on the geometric details of the motion, etc., all of which can potentially compromise the interpretation [32].

Despite the obvious limitations of the "oscillator inventory" approach, it has led to observations that promote the general idea that ligand binding to proteins produces significant changes in internal motion that, in turn, correspond to significant changes in conformational entropy (e.g., [72, 79–85]). We have used calmodulin and its multitude of binding partners as a model system to investigate the role of conformational entropy in high affinity association of proteins [86]. Calmodulin is central to calcium-mediated signal transduction pathways of eukaryotes [87] and interacts with hundreds of proteins with high affinity [88]. The structures of the calmodulin complexes generally follow a "hot dog in a bun" type of topology where the two globular domains of calmodulin collapse around the target calmodulin-binding domain, which forms an amphiphilic helix that is largely sequestered from solvent. Calmodulin-binding domains are generally 20–30 residue sequences characterized by enrichment in basic and hydrophobic residues [88]. This system is particularly amenable to deuterium methyl relaxation experiments [32, 72, 78, 86, 89, 90]. As shown in Fig. 4, methyl probes are distributed throughout the calmodulin molecule. The target domains also have strong representation by the methyl-bearing amino acids [89].
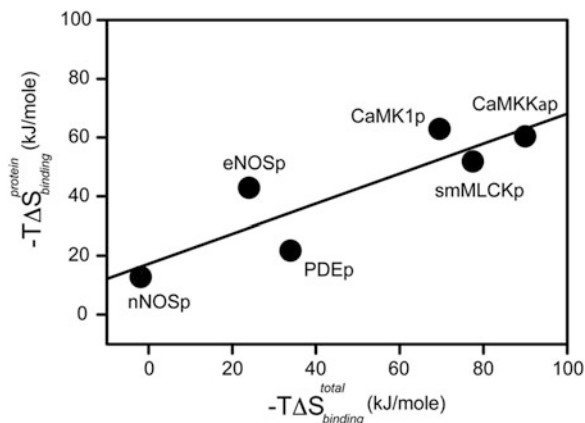
Fig. 5 Application of the oscillator inventory approach to the calmodulin complexes. CaM complexes with six natural target domains were employed. The change in conformational entropy was estimated from the changes in methyl group symmetry axis squared generalized order parameters measured by deuterium relaxation [86]. The simple harmonic oscillator model was used. The linear correlation coefficient (R^2) of conformational entropy vs the entropy of binding is 0.78. Adapted from Frederick et al. [86] with permission. Copyright Nature Publishing

Using NMR relaxation measurements, we have shown that calcium-saturated calmodulin (CaM) is an unusually dynamic protein that is characterized by a broad range of the amplitudes (i.e., order parameters) of fast side-chain dynamics that are redistributed upon binding of a CaM-binding domain of a regulated protein [72]. Particularly intriguing is the observation that the conformational entropy estimated by the "oscillator inventory" approach correlated linearly with the overall entropy of binding of a series of CaM-binding domains to CaM (Fig. 5) [86]. It must be emphasized that there is no physical law that requires a linear correlation of a single component of the total entropy (i.e., the conformational entropy) with the total entropy. However, the persistence of such a linear correlation suggests a biological origin: Nature employs conformational entropy in evolving toward the optimal free energy of binding. To first approximation this makes sense if a primary selection pressure for evolution of a protein–ligand interaction is the free energy of association then all sources of entropy will be invoked, to the extent possible, to satisfy this evolutionary demand.

5 Creation and Calibration of an "Entropy Meter"

A more recent approach is perhaps less assailable and more convincing than the simple "oscillator inventory." The idea is to subsume the various microscopic concerns enumerated above and find an *empirical* calibration. Thus measures of motion are used in a largely model-independent way, which thereby circumvents

the microscopic details that are difficult to accommodate in a model-dependent calculation. In a sense, we have simply created an "entropy meter," analogous to a thermometer. It is important to note that in this approach the motion of the methyl group is used to sense its local surroundings. This relies on the coupling of motion within the protein such that the "probe" methyl groups report on the local disorder [90]. This is a critical change in perspective where the dynamical probe is interpreted to reflect not only its own disorder but also the disorder of the surrounding non-probe protein matrix. Thus, for the approach to work there must be sufficient coupling between the motion of the probe and its surroundings and there must be a sufficient density of probes to provide adequate coverage of the protein.

5.1 Derivation of the Dynamical Proxy "Entropy Meter"

Making several simple assumptions regarding the nature of the free states so that the solvation entropy can be calculated, one can obtain in this case [90]

$$\Delta S_{\text{conf}} = m \left[\left(n_{\text{res}}^{\text{CaM}} \bullet \left\langle \Delta O_{\text{axis}}^2 \right\rangle^{\text{CaM}} + n_{\text{res}}^{\text{target}} \bullet \left\langle \Delta O_{\text{axis}}^2 \right\rangle^{\text{target}} \right) \right] + \Delta S_{\text{other}} \quad (5)$$

$$(\Delta S_{\text{tot}} - \Delta S_{\text{sol}}) = m \left[\left(n_{\text{res}}^{\text{CaM}} \bullet \left\langle \Delta O_{\text{axis}}^2 \right\rangle^{\text{CaM}} + n_{\text{res}}^{\text{target}} \bullet \left\langle \Delta O_{\text{axis}}^2 \right\rangle^{\text{target}} \right) \right] + \Delta S_{\text{RT}}$$
$$+ \Delta S_{\text{other}} \quad (6)$$

where ΔS_{tot}, ΔS_{sol}, ΔS_{conf}, ΔS_{RT}, and ΔS_{other} are the changes in total system entropy, solvent entropy, conformational entropy, rotational-translational entropy, and undocumented entropy, which is mostly solvent entropy from ion pair dissociation and solvation. The changes in side chain motion are assessed from changes in methyl order parameters weighted by the number of residues in calmodulin ($n_{\text{res}}^{\text{CaM}}$) and the target domains ($n_{\text{res}}^{\text{target}}$). By postulate, ΔS_{conf} is linearly related to the residue-weighted change in the dynamics of the target domain and the protein (e.g., calmodulin) upon binding. Linearity is strongly supported by the simple simulations illustrated in Fig. 3 [78]; "m" is the desired empirical scaling factor relating changes in motion to changes in conformation entropy.

ΔS_{tot} is obtained from isothermal titration calorimetry. ΔS_{sol} is obtained from the change in accessible surface area revealed by the structures of free CaM and the complexes. Despite some limitations of this particular system (see below), the approach worked very well. Figure 6 shows the empirical calibration of the "entropy meter" using five calmodulin complexes. The five complexes give an excellent linear relationship ($R = 0.95$) and a slope (m) of -0.037 ± 0.007 kJ K^{-1} mol res^{-1}.
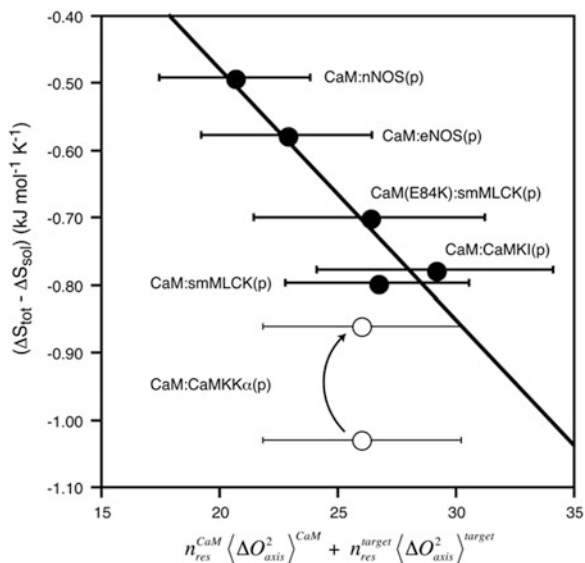
Fig. 6 Calibration of the dynamical proxy for protein conformational entropy. Simple considerations lead to the prediction of a quantitative linear relationship between the total binding entropy and the entropy of solvent to the conformational entropy by NMR relaxation parameters derived from methyl bearing amino acids (see (6)). The dynamics of free CaM and six CaM complexes were determined by deuterium methyl relaxation [89]. The lower CaM:CaMKKα(p) datum is a clear outlier, likely due to residual structure in the free CaMKKα(p) peptide. The upper CaM:CaMKKα(p) point results from a simple correction. Excluding the CaM:CaMKKα(p) complex gives the *regression line* shown. The slope of -0.037 ± 0.007 kJ K^{-1} mol res^{-1} allows for empirical calibration of the conversion of changes in side-chain dynamics to a quantitative estimate of changes in conformational entropy. The ordinate intercept is 0.26 ± 0.18 kJ K^{-1} mol res^{-1}. Reproduced with permission from Marlow et al. [89]. Copyright Nature Publishing

5.2 Quantitative Evaluation of Entropy in Molecular Recognition by Calmodulin

The calibration of the "entropy meter" allows the contribution of conformational entropy to the binding entropy to be evaluated quantitatively (Fig. 7). Scaling of observed changes in dynamics in calmodulin to real entropy units provides, for the first time, a quantitative statement of how changes in the conformational entropy of a protein contribute significantly to the overall binding free energy of a protein–ligand complex [90]. The basic result is striking: the conformational entropy of calmodulin is a significant component of the free energy of binding of the target domains. Indeed, the variation of the conformational entropy of calmodulin effectively "tunes" the binding entropy [89].

It is important to point out that this first example of empirical calibration of a dynamical "entropy meter" used a less than ideal system. First, access to the solvent entropy of binding relied on the assumption that the free target domains
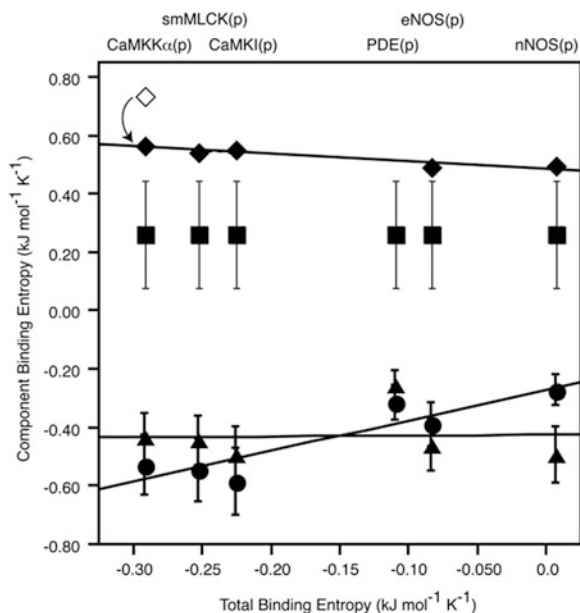
Fig. 7 Decomposition of the entropy of binding of target domains to calcium-saturated calmodulin. Based on (6) and the calibration of the dynamical proxy (see Fig. 6). *Solid diamonds* are the solvent entropies calculated from the changes in accessible surface area and include the correction resulting from the postulated hydrophobic cluster of the free CaMKα(p) target domain. The uncorrected value is shown as an *open diamond*. No structure is available for the CaM:PDE(p) complex so its solvent entropy cannot be calculated. *Solid circles* and *triangles* are the contributions to the binding entropy by the conformational entropy of CaM and the target domains, respectively. *Solid squares* are the contributions to the binding entropy not reflected in the measured dynamics (see (6)), which is obtained from linear regression. Reproduced with permission from Marlow et al. [89]. Copyright Nature Publishing

(represented as peptides) are fully solvated, i.e., completely random coil. This enabled determination of the accessible surface area of the free peptide ligand. As the CaMKKα(p) example illustrated, this is not always warranted. In addition, the calculation of solvent entropy does not consider the creation (or removal) of explicit charge. This is potentially an issue with the calmodulin complexes as each contains intimate and buried ion pairs bridging the components. It is also assumed that there are no differences in the contribution of rotation and conformational entropy to the binding free energy across the various complexes. Another important assumption is that the entropy of the free ligand can be represented by the dynamics of an unhindered methyl group. Undocumented variation in either $\Delta S_{\text{solvent}}$ or ΔS_{RT} or ΔS_{conf} of the ligand would tend to scatter the points. Fortunately, variation of these and other contributions assumed to be constant across the complexes was not a factor [except in the case of the CaMKKα(p) complex]. Nevertheless, it is clear that similar efforts are most ideally carried out on a series of complexes where ambiguity in solvation and rotational and translational entropy

is less worrisome. An example of the former approach is shown in Fig. 6 where a point mutant in CaM perturbs the thermodynamics of binding to provide a useful calibration point.

Because the calmodulin complexes represent the first example of the empirical dynamical entropy meter approach, it remains unknown whether or not the empirical scaling constant is generally applicable. It would be surprising if the fundamental nature of the protein molecule giving rise to the motional coupling underpinning the approach would vary dramatically. Nevertheless, modest variation would seem entirely possible and this issue awaits further exploration of additional systems.

5.3 Future Strategies

Though the first application of the empirical "entropy meter" approach employing a dynamical proxy was apparently successful, the use of the calmodulin system highlights several potential weaknesses. In the case of calmodulin complexes, the predominant strategy was to compare complexes of different ligand target domains. Though very similar in amino acid composition and size, this introduces uncertainty in the assumption that changes in solvent entropy can be adequately calculated and that rotational-translational entropy and other sources of entropy changes remain constant across the complexes. An alternative and presumably less problematic approach is illustrated by the lone mutant CaM complex examined (Fig. 6). By using mutants distant from the protein–ligand interface to perturb the overall entropy of binding (in part through perturbations of conformational entropy) one can carry out a calibration with the same ligand. Furthermore, if mutants are carefully chosen to avoid significant variation in structure then uncertainty in changes in rotational-translational and solvent entropy will be largely avoided. Finally, it is not yet clear how to combine different probe types. Though the simple averaging of different methyl bearing amino acid dynamics gives impressive results, one anticipates that a more sophisticated averaging reflecting the variation in degrees of freedom associated with a given methyl group should be employed. This type of consideration will be even more important as quite distinct dynamic probes are introduced (e.g., the large aromatic ring systems) to ensure adequate coverage.

6 Implications for Enzyme Catalysis

Notwithstanding the uncertainty regarding the universality of the empirical linear scaling between protein motion and conformational entropy, it is interesting to speculate what the impact of conformational entropy might be in the catalytic cycle of enzymes. Here we draw two examples from the literature: hen egg white lysozyme (HEWL) and its interaction with a natural inhibitor and *E. coli* dihydrofolate reductase (DHFR) and the transition from the binary complex to the ternary Michaelis complex.

6.1 *Conformational Entropy and Inhibitor Binding to Lysozyme*

HEWL was the first enzyme to have its three-dimensional structure determined by X-ray diffraction [92] and has since served as a paradigm for a wide-range of biochemical and biophysical studies. The double-displacement catalytic mechanism proposed initially by Koshland [93] involving a covalent intermediate with the substrate has supplanted [94] the long held Philips mechanism that centered on a long-lived oxocarbenium ion intermediate [92]. Here we examined the thermodynamics of the interaction of an inhibitory carbohydrate with HEWL. Lysozymes catalyze the hydrolysis of β-(1,4)-linkages between *N*-acetylmuramic acid and *N*-acetyl-D-glucosamine (GlcNAc) in peptidoglycans. Additionally, some lysozymes, including that from hen egg whites, can cleave between GlcNAc residues in chitodextrins such as chitin [95]. HEWL can accommodate up to six GlcNAc residues of a chitin polymer, each binding in six sub-sites along a cleft of the protein. Cleavage occurs at the linkage between the GlcNAc residues occupying the third and fourth subsites [94, 96] and thus does not readily occur with molecules consisting of only one (GlcNAc), two (chitobiose), or three (chitotriose) GlcNAc residues [97, 98]. These smaller molecules do, however, bind with reasonable affinity ($K_d \sim 10^{-4}$ to 10^{-6} M) [98, 99] and therefore act as natural competitive inhibitors. Using isothermal titration calorimetry, the binding of both chitobiose and chitotriose to HEWL has been found to be enthalpically driven over a wide range of temperatures [98]. The extent of the contribution from conformational entropy manifested as fast internal motion of the protein, however, is unclear, as indicated by (1). To examine this issue, we have recently carried out a comprehensive characterization of the sub-nanosecond time scale dynamics of the backbone and of the methyl-bearing side chains of HEWL in the apo state and in complex with chitotriose [100].

The fast sub-nanosecond dynamics of the backbone and the side chains were characterized using ^{15}N- and ^{2}H-methyl relaxation, respectively [100]. From the point of view of fast methyl-bearing side chain dynamics, HEWL is an unusually rigid protein in both its free and chitotriose complexed states. Of proteins that have been examined in this way, only those having high affinity cofactors (flavodoxin) or covalently attached prosthetic groups (cytochrome c and c_2) have comparable general rigidity [73, 101, 102]. There is no distinct spatial clustering of rigidity or flexibility in the molecular structure of either the free protein or its binary complex with chitotriose.

The response of the side chain motion to chitotriose binding is complex and heterogeneous, with some sites increasing the amplitude of their motion while others are decreased. Interestingly, a significant number of relatively rigid methyl-bearing side chains of the apo state effectively become completely immobile upon binding of the ligand. These residues form a contiguous grouping that spans the core of the protein including the two catalytic residues. This core of rigidification is capped by residues that are released from an effectively rigid state in the apo state to become more dynamic upon binding chitotriose (Fig. 8). This study appears to shed light on
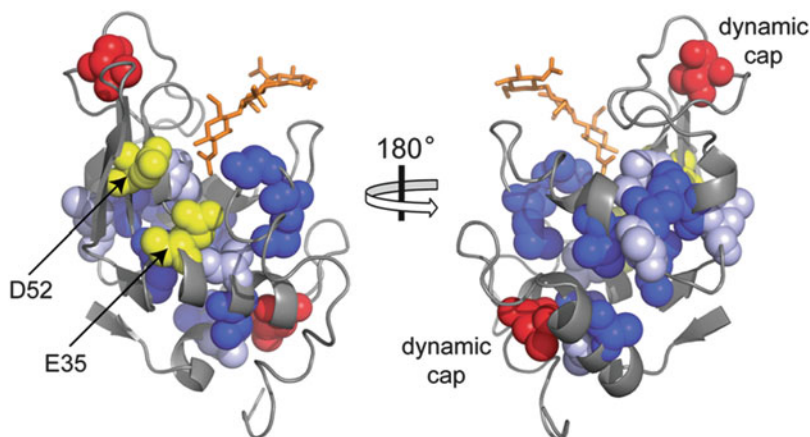
Fig. 8 Apparent cooperative rigidification of HEWL upon binding chitotriose. The backbone of the HEWL crystal structure [103] (PDB code 1LZB) is rendered as a *ribbon* and the chitotriose is shown as a *stick figure*. Atoms of residues whose methyl groups are effectively rigid in both the apo and complexed states (*light*) or become effectively rigid in the complexed state (*dark*) are shown as *spheres*. The atoms of residues whose methyl groups are effectively rigid in the apo state and become dynamic in the complex and cap the residues that are rigid in the bound state are indicated with *arrows*. The catalytic amino acids E35 and D52 are also labeled. Taken from Moorman et al. [100] with permission. Copyright Wiley-Blackwell and the Protein Society

a cooperatively formed rigidified core contacting HEWL's catalytic residues and capped by two sites that become markedly more flexible on either end. The changes in methyl axis squared generalized order parameters across the molecule average to nearly zero ($\Delta O^2_{\text{axis}} = +0.019 \pm 0.004$). If it is assumed that the empirical scaling between changes in motion and the corresponding changes in conformational entropy determined for the calmodulin complexes [89] is applicable, then by averaging over the entire lysozyme protein and scaling the resulting average change in ΔO^2_{axis} with the empirical constant of -0.037 ± 0.007 kJ mol res^{-1} K^{-1} one estimates that the response of lysozyme to binding of chitotriose corresponds to $+28 \pm 8$ kJ mol^{-1} at 308 K.

6.2 Conformational Entropy and Dihydrofolate Reductase

Dihydrofolate reductase (DHFR) is a ubiquitous enzyme found in all organisms. It catalyzes the hydride transfer reaction converting dihydrofolate (DHF) to tetrahydrofolate using NADPH as its reducing cofactor. This enzyme is solely responsible for the cellular supply of THF, which serves as an essential metabolic precursor for DNA biosynthesis [104]. The catalytic cycle involves five intermediates, all of which involve at least one bound ligand. Following the hydride transfer step, the protein undergoes a conformational change in an active site loop

Fig. 9 *Ribbon* diagram of the
E. coli DHFR enzyme in
complex with NADP^{+} and
folate. Drawn with PyMol
(Schrödinger, Portland,
Oregon). Based on PDB code
1RX2 [108]
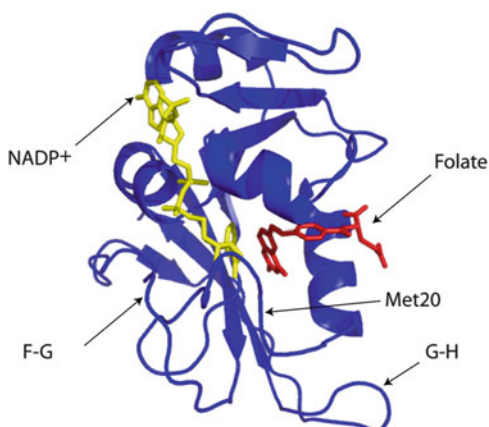
referred to as the Met 20 loop (Fig. 9). This loop moves from the closed state, in
which it shields the reactants from solvent, to the occluded state, where the nicotin-
amide ring of NADPH is blocked from the active site. Two other proximal loops, the
F–G and G–H loops, stabilize the two states of the Met 20 loop through hydrogen
bonding interactions [104]. The dynamics of these loops appears to play an important
role in catalysis [105]. Studies of sub-nanosecond side chain dynamics of DHFR have
also been performed and show significant changes in methyl order parameters during
different stages of the catalytic cycle [106]. An interesting example impacts our
understanding of the role of conformational entropy during the catalytic cycle.
Wright and coworkers [106] determined the Lipari–Szabo methyl symmetry axis
order parameters of *E. coli* DHFR ternary complex with NADP^{+} and folate, which is
a generally accepted model for the DHFR·NADPH·dihydrofolate Michaelis com-
plex. Lee and coworkers [107] have carried out a similar study of the DHFR·NADPH
binary complex. Though done under slightly different experimental conditions (T,
pH, buffer), the average change in O^2_{axis} of about $+0.02$ on going from the binary to
the ternary complex combined with the scaling constant of Marlow et al. [89]
suggests that an unfavorable reduction in entropy of ~0.1 kJ mol^{-1} K^{-1} in confor-
mational entropy of DHFR accompanies binding of dihydrofolate to form the ternary
DHFR·NADPH·dihydrofolate complex. This would correspond to a very unfavorable
contribution to the free energy of dihydrofolate binding of roughly $+30$ kJ/mol^{-1} at
300 K. This result begins to suggest that conformational entropy can have significant
impact in the interconversion of kinetic intermediates during enzyme catalysis.

7   Conclusions

The application of NMR relaxation to fundamental issues in enzymology is now
reaching into the thermodynamic origins of enzyme catalysis. The development of
powerful experimental strategies now allows for the measurement of fast internal

dynamics of proteins in various functional states and contexts. The experimental and analytical strategies needed to employ measures of motion as a proxy for the underlying conformational entropy of proteins have begun to mature. Tantalizing new features of both protein motion and the role of conformational entropy in protein function are emerging. Indeed, in the few examples of ligand binding to enzymes studied to date, the role of conformational entropy in defining the energetics of product release appears significant and warrants further detailed examination of other systems. It seems clear that these types of insights are likely not only to impact our general understanding of enzymatic function but also to assist in the more robust design of pharmaceuticals directed against them.

References

1. Fischer E (1894) Einfluss der confriuation auf die Wirkung der enzyme. Ber Dt Chem Ges 27:2895–2993
2. Koshland DE (1958) Application of a theory of enzyme specificity to protein synthesis. Proc Natl Acad Sci USA 44:98–104
3. Bosshard HR (2001) Molecular recognition by induced fit: how fit is the concept? News Phys Sci 16:171–173
4. Tsai CJ, Ma B, Nussinov R (1999) Folding and binding cascades: shifts in energy landscapes. Proc Natl Acad Sci USA 96:9970–9972
5. Frauenfelder H, Sligar SG, Wolynes PG (1991) The energy landscapes and motions of proteins. Science 254:1598–1603
6. Hilser VJ, Garcia-Moreno EB, Oas TG, Kapp G, Whitten ST (2006) A statistical thermodynamic model of the protein ensemble. Chem Rev 106:1545–1558
7. Henzler-Wildman K, Kern D (2007) Dynamic personalities of proteins. Nature 450:965–972
8. Wolynes PG (2005) Recent successes of the energy landscape theory of protein folding and function. Q Rev Biophys 38:405–410
9. Volkman BF, Lipson D, Wemmer DE, Kern D (2001) Two-state allosteric behavior in a single-domain signaling protein. Science 291:2429–2433
10. Boehr DD, McElheny D, Dyson HJ, Wright PE (2006) The dynamic energy landscape of dihydrofolate reductase catalysis. Science 313:1638–1642
11. Eisenmesser EZ, Bosco DA, Akke M, Kern D (2002) Enzyme dynamics during catalysis. Science 295:1520–1523
12. Eisenmesser EZ, Millet O, Labeikovsky W, Korzhnev DM, Wolf-Watz M, Bosco DA, Skalicky JJ, Kay LE, Kern D (2005) Intrinsic dynamics of an enzyme underlies catalysis. Nature 438:117–121
13. Fraser JS, Clarkson MW, Degnan SC, Erion R, Kern D, Alber T (2009) Hidden alternative structures of proline isomerase essential for catalysis. Nature 462:669, 673
14. Bhabha G, Lee J, Ekiert DC, Gam J, Wilson IA, Dyson HJ, Benkovic SJ, Wright PE (2011) A dynamic knockout reveals that conformational fluctuations influence the chemical step of enzyme catalysis. Science 332:234–238
15. Kamerlin SCL, Warshel A (2010) At the dawn of the 21st century: is dynamics the missing link for understanding enzyme catalysis? Proteins 78:1339–1375

16. Doshi U, McGowan LC, Ladani ST, Hamelberg D (2012) Resolving the complex role of enzyme conformational dynamics in catalytic function. Proc Natl Acad Sci USA 109 (15):5699–5704
17. Dill KA (1990) Dominant forces in protein folding. Biochemistry 29:7133–7154
18. Gilson MK, Given JA, Bush BL, McCammon JA (1997) The statistical-thermodynamic basis for computation of binding affinities: a critical review. Biophys J 72:1047–1069
19. Gilson MK, Zhou HX (2007) Calculation of protein-ligand binding affinities. Annu Rev Biophys Biomol Struct 36:21–42
20. Zhou HX, Gilson MK (2009) Theory of free energy and entropy in noncovalent binding. Chem Rev 109:4092–4107
21. Homans SW (2007) Water, water everywhere – except where it matters? Drug Discov Today 12:534–539
22. Doyle ML (1997) Characterization of binding interactions calorimetry. Curr Opin Biotechnol 8:31–35
23. Tanford C (1978) The hydrophobic effect and the organization of living matter. Science 200:1012–1018
24. Sharp KA, Nicholls A, Fine RF, Honig B (1991) Reconciling the magnitude of the microscopic and macroscopic hydrophobic effects. Science 252:106–109
25. Chandler D (2005) Interfaces and the driving force of hydrophobic assembly. Nature 437:640–647
26. Steinberg IZ, Scheraga HA (1963) Entropy changes accompanying association reactions of proteins. J Biol Chem 238:172–181
27. Cooper A (1976) Thermodynamic fluctuations in protein molecules. Proc Natl Acad Sci USA 73:2740–2741
28. Levitt M, Warshel A (1975) Computer simulation of protein folding. Nature 253:694–698
29. McCammon JA, Gelin BR, Karplus M (1977) Dynamics of folded proteins. Nature 267:585–590
30. Frauenfelder H, Petsko GA, Tsernoglou D (1979) Temperature-dependent X-ray diffraction as a probe of protein structural dynamics. Nature 280:558–563
31. Gurd FR, Rothgeb TM (1979) Motions in proteins. Adv Protein Chem 33:73–165
32. Igumenova TI, Frederick KK, Wand AJ (2006) Characterization of the fast dynamics of protein amino acid side chains using NMR relaxation in solution. Chem Rev 106:1672–1699
33. Karplus M, Ichiye T, Pettitt BM (1987) Configurational entropy of native proteins. Biophys J 52:1083–1085
34. Li Z, Raychaudhuri S, Wand AJ (1996) Insights into the local residual entropy of proteins provided by NMR relaxation. Protein Sci 5:2647–2650
35. Palmer AG, Massi F (2006) Characterization of the dynamics of biomacromolecules using rotating-frame spin relaxation NMR spectroscopy. Chem Rev 106:1700–1719
36. Jarymowycz VA, Stone MJ (2006) Fast time scale dynamics of protein backbones: NMR relaxation methods, applications, and functional consequences. Chem Rev 106:1624–1671
37. Bai YW (2006) Protein folding pathways studied by pulsed-and native-state hydrogen exchange. Chem Rev 106:1757–1768
38. Ottiger M, Bax A (1998) Determination of relative N-H-NN-C′, C-alpha-C′, and C(alpha)-H-alpha effective bond lengths in a protein by NMR in a dilute liquid crystalline phase. J Am Chem Soc 120:12334–12341
39. Henry ER, Szabo A (1985) Influence of vibrational motion on solid-state line-shapes and NMR relaxation. J Chem Phys 82:4753–4761
40. Ferrage F, Pelupessy P, Cowburn D, Bodenhausen G (2006) Protein backbone dynamics through C-13′-C-13(alpha) cross-relaxation in NMR spectroscopy. J Am Chem Soc 128:11072–11078
41. Liu WD, Zheng Y, Cistola DP, Yang DW (2003) Measurement of methyl C-13-H-1 cross-correlation in uniformly C-13-, N-15-, labeled proteins. J Biomol NMR 27:351–364

42. Pelupessy P, Ravindranathan S, Bodenhausen G (2003) Correlated motions of successive amide N-H bonds in proteins. J Biomol NMR 25:265–280
43. Vugmeyster L, Pelupessy P, Vugmeister BE, Abergel D, Bodenhausen G (2004) Cross-correlated relaxation in NMR of macromolecules in the presence of fast and slow internal dynamics. C R Phys 5:377–386
44. Wang TZ, Frederick KK, Igumenova TI, Wand AJ, Zuiderweg ERP (2005) Changes in calmodulin main-chain dynamics upon ligand binding revealed by cross-correlated NMR relaxation measurements. J Am Chem Soc 127:828–829
45. Zhang X, Sui XG, Yang DW (2006) Probing methyl dynamics from C-13 autocorrelated and cross-correlated relaxation. J Am Chem Soc 128:5073–5081
46. Cavanagh J, Fairbrother WJ, Palmer AG, Rance M, Skelton NJ (2006) Protein NMR spectroscopy: principles and practice. Elsevier, Burlington, MA
47. Lipari G, Szabo A (1982) Model-free approach to the interpretation of nuclear magnetic-resonance relaxation in macromolecules. 1. Theory and range of validity. J Am Chem Soc 104:4546–4559
48. Lipari G, Szabo A (1982) Model-free approach to the interpretation of nuclear magnetic-resonance relaxation in macromolecules. 2. Analysis of experimental results. J Am Chem Soc 104:4559–4570
49. Tjandra N, Feller SE, Pastor RW, Bax A (1995) Rotational diffusion anisotropy of human ubiquitin from N-15 NMR relaxation. J Am Chem Soc 117:12562–12566
50. Lee LK, Rance M, Chazin WJ, Palmer AG (1997) Rotational diffusion anisotropy of proteins from simultaneous analysis of N-15 and C-13(alpha) nuclear spin relaxation. J Biomol NMR 9:287–298
51. Pawley NH, Wang C, Koide S, Nicholson LK (2001) An improved method for distinguishing between anisotropic tumbling and chemical exchange in analysis of 15N relaxation parameters. J Biomol NMR 20:149–165
52. Kneller JM, Lu M, Bracken C (2002) An effective method for the discrimination of motional anisotropy and chemical exchange. J Am Chem Soc 124:1852–1853
53. Mandel AM, Akke M, Palmer AG (1995) Backbone dynamics of *Escherichia coli* ribonuclease H1 – correlations with structure and function in an active enzyme. J Mol Biol 246:144–163
54. McIntosh LP, Dahlquist FW (1990) Biosynthetic incorporation of N15 and C13 for assignment and interpretation of nuclear magnetic resonance spectra of proteins. Q Rev Biophys 23:1–38
55. Wand AJ, Bieber RJ, Urbauer JL, McEvoy RP, Gan ZH (1995) Carbon relaxation in randomly fractionally C13 enriched proteins. J Magn Reson B 108:173–175
56. LeMaster DM, Kushlan DM (1996) Dynamical mapping of *E. coli* thioredoxin via C-13 NMR relaxation analysis. J Am Chem Soc 118:9255–9264
57. Lee AL, Urbauer JL, Wand AJ (1997) Improved labeling strategy for C-13 relaxation measurements of methyl groups in proteins. J Biomol NMR 9:437–440
58. Gardner KH, Kay LE (1998) The use of H-2, C-13, N-15 multidimensional NMR to study the structure and dynamics of proteins. Annu Rev Biophys Biomol Struct 27:357–406
59. Goto NK, Gardner KH, Mueller GA, Willis RC, Kay LE (1999) A robust and cost-effective method for the production of Val, Leu, Ile (delta 1) methyl-protonated N-15-, C-13-, H-2-labeled proteins. J Biomol NMR 13:369–374
60. Ollerenshaw JE, Tugarinov V, Skrynnikov NR, Kay LE (2005) Comparison of (CH3)-C-13, (CH2D)-C-13, and (CHD2)-C-13 methyl labeling strategies in proteins. J Biomol NMR 33:25–41
61. Kay LE, Torchia DA, Bax A (1989) Backbone dynamics of proteins as studied by N-15 inverse detected heteronuclear NMR spectroscopy – application to staphylococcal nuclease. Biochemistry 28:8972–8979
62. Farrow NA, Muhandiram R, Singer AU, Pascal SM, Kay CM, Gish G, Shoelson SE, Pawson T, Formankay JD, Kay LE (1994) Backbone dynamics of a free and a

phosphopeptide-complexed Src homology-2 domain studied by N-15 NMR relaxation. Biochemistry 33:5984–6003

63. Muhandiram DR, Yamazaki T, Sykes BD, Kay LE (1995) Measurement of H-2T-1 and T-1p relaxation-times in uniformly C-13-labeled and fractionally H-2-labeled proteins in solution. J Am Chem Soc 117:11536–11544

64. Millet O, Muhandiram DR, Skrynnikov NR, Kay LE (2002) Deuterium spin probes of side-chain dynamics in proteins. 1. Measurement of five relaxation rates per deuteron in C-13-labeled and fractionally H-2-enriched proteins in solution. J Am Chem Soc 124:6439–6448

65. Tugarinov V, Kay LE (2005) Quantitative 13C and 2H NMR relaxation studies of the 723-residue enzyme malate synthase G reveal a dynamic binding interface. Biochemistry 44:15970–15977

66. Liao X, Long D, Li DW, Bruschweiler R, Tugarinov V (2012) Probing side-chain dynamics in proteins by the measurement of nine deuterium relaxation rates per methyl group. J Phys Chem B 116:606–620

67. Ishima R, Petkova AP, Louis JM, Torchia DA (2001) Comparison of methyl rotation axis order parameters derived from model-free analyses of H-2 and C-13 longitudinal and transverse relaxation rates measured in the same protein sample. J Am Chem Soc 123:6164–6171

68. Dellwo MJ, Wand AJ (1989) Model-independent and model-dependent analysis of the global and internal dynamics of cyclosporine-A. J Am Chem Soc 111:4571–4578

69. Tjandra N, Kuboniwa H, Ren H, Bax A (1995) Rotational dynamics of calcium-free calmodulin studied by 15N-NMR relaxation measurements. Eur J Biochem 230:1014–1024

70. Wand AJ, Urbauer JL, McEvoy RP, Bieber RJ (1996) Internal dynamics of human ubiquitin revealed by C-13-relaxation studies of randomly fractionally labeled protein. Biochemistry 35:6116–6125

71. Ishima R, Louis JM, Torchia DA (2001) Optimized labeling of (CHD2)-C-13 methyl isotopomers in perdeuterated proteins: potential advantages for C-13 relaxation studies of methyl dynamics of larger proteins. J Biomol NMR 21:167–171

72. Lee AL, Kinnear SA, Wand AJ (2000) Redistribution and loss of side chain entropy upon formation of a calmodulin-peptide complex. Nat Struct Biol 7:72–77

73. Liu W, Flynn PF, Fuentes EJ, Kranz JK, McCormick M, Wand AJ (2001) Main chain and side chain dynamics of oxidized flavodoxin from cyanobacterium Anabaena. Biochemistry 40:14744–14753

74. Walsh ST, Lee AL, DeGrado WF, Wand AJ (2001) Dynamics of a de novo designed three-helix bundle protein studied by 15N, 13C, and 2H NMR relaxation methods. Biochemistry 40:9560–9569

75. Akke M, Bruschweiler R, Palmer AG (1993) NMR order parameters and free-energy – an analytical approach and its application to cooperative Ca2+ binding by calbindin-D(9 k). J Am Chem Soc 115:9832–9833

76. Yang D, Kay LE (1996) Contributions to conformational entropy arising from bond vector fluctuations measured from NMR-derived order parameters: application to protein folding. J Mol Biol 263:369–382

77. Privalov PL, Gill SJ (1988) Stability of protein structure and hydrophobic interaction. Adv Protein Chem 39:191–234

78. Lee AL, Sharp KA, Kranz JK, Song XJ, Wand AJ (2002) Temperature dependence of the internal dynamics of a calmodulin-peptide complex. Biochemistry 41:13814–13825

79. Law AB, Fuentes EJ, Lee AL (2009) Conservation of side-chain dynamics within a protein family. J Am Chem Soc 131:6322–6323

80. Clarkson MW, Gilmore SA, Edgell MH, Lee AL (2006) Dynamic coupling and allosteric behavior in a nonallosteric protein. Biochemistry 45:7693–7699

81. Clarkson MW, Lee AL (2004) Long-range dynamic effects of point mutations propagate through side chains in the serine protease inhibitor Eglin c. Biochemistry 43:12448–12458

82. Fuentes EJ, Der CJ, Lee AL (2004) Ligand-dependent dynamics and intramolecular signaling in a PDZ domain. J Mol Biol 335:1105–1115
83. Fuentes EJ, Gilmore SA, Mauldin RV, Lee AL (2006) Evaluation of energetic and dynamic coupling networks in a PDZ domain protein. J Mol Biol 364:337–351
84. Popovych N, Tzeng SR, Tonelli M, Ebright RH, Kalodimos CG (2009) Structural basis for cAMP-mediated allosteric control of the catabolite activator protein. Proc Natl Acad Sci USA 106:6927–6932
85. Tzeng SR, Kalodimos CG (2009) Dynamic activation of an allosteric regulatory protein. Nature 462:368–372
86. Frederick KK, Marlow MS, Valentine KG, Wand AJ (2007) Conformational entropy in molecular recognition by proteins. Nature 448:325–329
87. Kahl CR, Means AR (2003) Regulation of cell cycle progression by calcium/calmodulin-dependent pathways. Endocr Rev 24:719–736
88. Yap KL, Kim J, Truong K, Sherman M, Yuan T, Ikura M (2000) Calmodulin target database. J Struct Funct Genomics 1:8–14
89. Marlow MS, Dogan J, Frederick KK, Valentine KG, Wand AJ (2010) The role of conformational entropy in molecular recognition by calmodulin. Nat Chem Biol 6:352–358
90. Marlow MS, Wand AJ (2006) Conformational dynamics of calmodulin in complex with the calmodulin-dependent kinase kinase alpha calmodulin-binding domain. Biochemistry 45:8732–8741
91. Frederick KK, Kranz JK, Wand AJ (2006) Characterization of the backbone and side chain dynamics of the CaM-CaMKIp complex reveals microscopic contributions to protein conformational entropy. Biochemistry 45:9841–9848
92. Blake CCF, Koenig DF, Mair GA, North ACT, Phillips DC, Sarma VR (1965) Structure of hen egg-white lysozyme – a 3-dimensional Fourier synthesis at 2 Å resolution. Nature 206:757–761
93. Koshland DE (1953) Stereochemistry and the mechanism of enzymatic reactions. Biol Rev Camb Philos Soc 28:416–436
94. Vocadlo DJ, Davies GJ, Laine R, Withers SG (2001) Catalysis by hen egg-white lysozyme proceeds via a covalent intermediate. Nature 412:835–838
95. Berger LR, Weiser RS (1957) The beta-glucosaminidase activity of egg-white lysozyme. Biochim Biophys Acta 26:517–521
96. Blake CC, Johnson LN, Mair GA, North AC, Phillips DC, Sarma VR (1967) Crystallographic studies of the activity of hen egg-white lysozyme. Proc R Soc Lond B Biol Sci 167:378–388
97. Rupley JA (1964) The hydrolysis of chitin by concentrated hydrochloric acid, and the preparation of low-molecular-weight substrates for lysozyme. Biochim Biophys Acta 83:245–255
98. Garcia-Hernandez E, Zubillaga RA, Chavelas-Adame EA, Vazquez-Contreras E, Rojo-Dominguez A, Costas M (2003) Structural energetics of protein-carbohydrate interactions: insights derived from the study of lysozyme binding to its natural saccharide inhibitors. Protein Sci 12:135–142
99. Laible NJ, Germaine GR (1985) Bactericidal activity of human lysozyme, muramidase-inactive lysozyme, and cationic polypeptides against *Streptococcus sanguis* and *Streptococcus faecalis* – inhibition by chitin oligosaccharides. Infect Immun 48:720–728
100. Moorman VR, Valentine KG, Wand AJ (2012) The dynamical response of hen egg white lysozyme to the binding of a carbohydrate ligand. Protein Sci 21(7):1066–1073
101. Liu W, Rumbley JN, Englander SW, Wand AJ (2009) Fast structural dynamics in reduced and oxidized cytochrome c. Protein Sci 18:670–674
102. Flynn PF, Bieber Urbauer RJ, Zhang H, Lee AL, Wand AJ (2001) Main chain and side chain dynamics of a heme protein: 15N and 2H NMR relaxation studies of *R. capsulatus* ferrocytochrome c2. Biochemistry 40:6559–6569

103. Maenaka K, Matsushima M, Song H, Sunada F, Watanabe K, Kumagai I (1995) Dissection of protein-carbohydrate interactions in mutant hen egg-white lysozyme complexes and their hydrolytic activity. J Mol Biol 247:281–293
104. Schnell JR, Dyson HJ, Wright PE (2004) Structure, dynamics, and catalytic function of dihydrofolate reductase. Annu Rev Biophys Biomol Struct 33:119–140
105. Epstein DM, Benkovic SJ, Wright PE (1995) Dynamics of the dihydrofolate reductase-folate complex: catalytic sites and regions known to undergo conformational change exhibit diverse dynamical features. Biochemistry 34:11037–11048
106. Schnell JR, Dyson HJ, Wright PE (2004) Effect of cofactor binding and loop conformation on side chain methyl dynamics in dihydrofolate reductase. Biochemistry 43:374–383
107. Mauldin RV, Carroll MJ, Lee AL (2009) Dynamic dysfunction in dihydrofolate reductase results from antifolate drug binding: modulation of dynamics within a structural state. Structure 17:386–394
108. Sawaya MR, Kraut J (1997) Loop and subdomain movements in the mechanism of *Escherichia coli* dihydrofolate reductase: crystallographic evidence. Biochemistry 36:586–603